Biosensors and Bioelectronics 35 (2012) 342–348

Contents lists available at SciVerse ScienceDirect

Biosensors and Bioelectronics

journal homepage: www.elsevier.com/locate/bios

Sensitive detection of unlabeled oligonucleotides using a paired surface plasma waves biosensor

Ying-Chang Li[a,b], Chiuan-Chian Chiou[c], Ji-Dung Luo[c], Wei-Ju Chen[b], Li-Chen Su[a,b], Ying-Feng Chang[b,d], Yu-Sun Chang[d,e], Chao-Sung Lai[f,g], Cheng-Chung Lee[a], Chien Chou[a,b,g,*]

[a] Department of Optics and Photonics, National Central University, Taoyuan, 320, Taiwan
[b] Graduate Institute of Electro-Optical Engineering, Chang Gung University, Taoyuan, 333, Taiwan
[c] Department of Medical Biotechnology and Laboratory Science, Chang Gung University, Taoyuan, 333, Taiwan
[d] Molecular Medicine Research Center, Chang Gung University, Taoyuan, 333, Taiwan
[e] Graduate Institute of Biomedical Sciences, Chang Gung University, Taoyuan, 333, Taiwan
[f] Department of Electronic Engineering, Chang Gung University, Taoyuan, 333, Taiwan
[g] Biomedical Engineering Research Center, Chang Gung University, Taoyuan, 333, Taiwan

ARTICLE INFO

Article history:
Received 10 January 2012
Received in revised form 8 March 2012
Accepted 9 March 2012
Available online 17 March 2012

Keywords:
Surface plasmon resonance
Hybridization

ABSTRACT

Detection of unlabeled oligonucleotides using surface plasmon resonance (SPR) is difficult because of the oligonucleotides' relatively lower molecular weight compared with proteins. In this paper, we describe a method for detecting unlabeled oligonucleotides at low concentration using a paired surface plasma waves biosensor (PSPWB). The biosensor uses a sensor chip with an immobilized probe to detect a target oligonucleotide via sequence-specific hybridization. PSPWB measures the demodulated amplitude of the heterodyne signal in real time. In the meantime, the ratio of the amplitudes between the detected output signal and reference can reduce the excess noise from the laser intensity fluctuation. Also, the common-path propagation of *p* and *s* waves cancels the common phase noise induced by temperature variation. Thus, a high signal-to-noise ratio (SNR) of the heterodyne signal is detected. The sequence specificity of oligonucleotide hybridization ensures that the platform is precisely discriminating between target and non-target oligonucleotides. Under optimized experimental conditions, the detected heterodyne signal increases linearly with the logarithm of the concentration of target oligonucleotide over the range 0.5–500 pM. The detection limit is 0.5 pM in this experiment. In addition, the non-target oligonucleotide at concentrations of 10 pM and 10 nM generated signals only slightly higher than background, indicating the high selectivity and specificity of this method. Different length of perfectly matched oligonucleotide targets at 10-mer, 15-mer and 20-mer were identified at the concentration of 150 pM.

1. Introduction

Surface plasmons (SP), a phenomenon arising from collective electron oscillations on a metal-dielectric interference, is of crucial interest in the field of modern optics. In view of its unique electromagnetic and optical properties in the near-field domain, the effective refractive index (n_{eff}) adjacent to a gold surface can be determined over a range of less than a few hundred nanometers. Since it measures the change of n_{eff}, including the refractive index and thickness of active medium close to gold surface, surface plasmon resonance (SPR) has been applied to real-time monitoring of biomolecular interactions, such as protein–protein (Hiep et al., 2010; Wong et al., 2008; Kuo et al., 2011), protein–DNA (Wu et al., 2007; Pollet et al., 2009; Tsoi and Yang, 2004; Majka and Speck, 2007; Wegner et al., 2003; Shumaker-Parry et al., 2004; Su et al., 2008; Luan et al., 2010), and drug–target interactions (Raz et al., 2009; Chiang et al., 2009). In nucleic acid research, the SPR biosensor has been widely applied to the quantitative detection of nucleic acids (Nelson et al., 2001; Halpern et al., 2011; Yu et al., 2009; Endo et al., 2010; Kick et al., 2010; Liu et al., 2008; Lin et al., 2010) and mutations (Ananthanawat et al., 2009; Carrascosa et al., 2009; Okumura et al., 2005; Jiang et al., 2005; Gorshkova et al., 2001; Milkani et al., 2010; Wang et al., 2009; D'Agata et al., 2008) because of its capability and sensitivity of dynamic detection for the study of binding kinetics. This technique has potential uses for the diagnosis of pathogens, metabolic pathways and genomic diseases.

Recently, the detection of DNA or RNA is becoming increasingly important in biomedical research and clinical applications. However, when applying SPR to the detection of oligonucleotide species, such as microRNA, the detection sensitivity is not satisfactory, as the signal intensity of SPR is highly dependent on the molecular weight of target analytes. Some post-hybridization labeling

* Corresponding author. Tel.: +886 3 2118800x3677; fax: +886 3 2118507.
E-mail address: cchou@mail.cgu.edu.tw (C. Chou).

0956-5663/$ – see front matter © 2012 Elsevier B.V. All rights reserved.
doi:10.1016/j.bios.2012.03.014

designs have been proposed to overcome this disadvantage, for example the use of a monoclonal antibody to bind RNA–DNA duplexes to increase mass on the sensor chip (Šípová et al., 2010), or post-labeling the oligonucleotide analytes with gold nanoparticles (Wark et al., 2007; Storhoff et al., 2004; D'Agata et al., 2010; Gifford et al., 2010). These post-hybridization labeling techniques allow for the sensitive detection of unlabeled oligonucleotides. However, these techniques require additional manipulation steps during experimental procedures, which may lead to increased cost, longer turn-around time, and the introduction of non-specific signals.

In order to retain advantages of an SPR-based platform with its label-free direct screening of small molecular interactions in the SPR-based platform, we propose a biosensor consisting of a paired surface plasma waves biosensor (PSPWB) (Kuo et al., 2003; Chou et al., 2006; Su et al., 2010), which integrates an intensity-based SPR technique and a common-path optical heterodyne interferometer. This setup focuses on real-time monitoring using an amplitude-ratio detection mode to reduce systematic noise and simultaneously improve the detection sensitivity outperforming conventional SPR biosensors. Our previous reports have demonstrated that PSPWB can detect sucrose at a concentration as low as 0.00001% (w/v) in DI water, which is equivalent to $\Delta n_{\text{eff}} = 1.4 \times 10^{-8}$ refractive index unit (RIU). The platform has been applied to detect total prostate-specific antigens in phosphate buffered saline, with a detection limit of 10 fg/mL (Su et al., 2010).

In this paper, the PSPW-based platform was set up for the sensitive detection of oligonucleotides. A single-strand oligonucleotide immobilized on the chip was used as a probe for detecting complementary oligonucleotides. The ultra-sensitive PSPWB platform allows for the detection of target oligonucleotides at a concentration of 0.5 pM without the need of labeling or post-labeling steps.

2. Experimental procedures

2.1. Materials

Immobilization buffer (10 mM sodium acetate, pH 5.0) and amine coupling kit, including 1-ethyl-3-(3-dimethylaminopropyl)-carbodiimide hydrochloride (EDC), N-hydroxysuccinimide (NHS), and 1.0 M ethanolamine-HCl (pH 8.5), were purchased from Biacore (Piscataway, NJ, USA). Phosphate buffered saline (PBS), 11-mercaptoundencanoic acid (11-MUA), 6-mercapto-1-hexanol (MCH) and streptavidin (SA) were purchased from Sigma–Aldrich (St. Louis, MO, USA). 2-Propanol was purchased from J.T. Baker (Phillipsburg, NJ, USA). Absolute ethanol and acetone were purchased from Mallinckrodt Baker (Paris, KY, USA).

Synthesized single-strand oligonucleotides treated with OPC-grade purification were purchased from Purigo (Taipei, Taiwan). Stock solution of the oligonucleotides (100 mM in PBS) was stored at −20 °C. Working solutions at various concentrations were diluted from the stock solution with PBS. Sequences and modification of the oligonucleotides are described in Table 1. The detection was conducted at 25 °C in PBS, which contains 10 mM sodium phosphate (pH 7.4) and 150 mM NaCl. (Table 1 is preferred at this position)

Table 1
Sequences and modification of oligonucleotides.

Oligonucleotides	Sequences (5′ → 3′)
Capture probe	
Biotin probe	5′-biotin-TCC CTC TGA TTA TGT TTA TTT AT-3′
Thiol probe	5′-SH-TCC CTC TGA TTA TGT TTA TTT AT-3′
Target	
T_{10}	5′-ATA AAT AAA C-3′
T_{15}	5′-ATA AAT AAA CAT AAT-3′
T_{20}	5′-ATA AAT AAA CAT AAT CAG AG-3′
Non-target	
NT_{23}	5′-TCC CTC TGA TTA TGT TTA TTT AT-3

2.2. PSPWB measurements

A single channel PSPWB (Fig.S1 in Supplementary information), was setup for oligonucleotide detection. PSPWB has the capability for noise reduction based on common-path geometry and optical heterodyne (Kuo et al., 2003; Chou et al., 2006; Su et al., 2010). The laser beam excites a pair of highly correlated surface plasma waves simultaneously. Two heterodyne signals ($P_1 + P_2$ and $S_1 + S_2$ waves) of equal beat frequency are generated in a polarized common-path interferometer. The *P* polarized wave (the signal beam) and *S* polarized wave (the reference beam) are detected by two photo detectors simultaneously so that phase and amplitude can be obtained by using a lock-in amplifier. In these measurements, the detection area is 1 mm^2 where we used a high quality lens with a focal length of 10 cm in order to focus the laser beam onto detector properly. The working principle and detailed description of PSPWB are given in Supplementary information.

2.3. Immobilization of oligonucleotide probes

SPR sensor chips were prepared by depositing 25.4 mm × 25.4 mm × 1 mm BK7 glass slides (Schott Glass) with a 2-nm adhesion layer of chromium followed by a 45-nm gold layer by electron beam evaporation. The chips were consecutively rinsed with acetone, 2-propanol and water then blown dry with nitrogen gas before use.

For surface functionalization, two main approaches for immobilizing oligonucleotide probes were conducted in these measurements. The first approach involved binding 11-MUA and streptavidin–biotin cross-linkers onto the gold surface whereas a self-assembled monolayer (SAM) was attached by immersing the cleaned SPR chip in a solution of absolute ethanol containing 1 mM 11-MUA for 24 h. After assembly, the chip was washed with absolute ethanol and distilled water, then dried with nitrogen gas. The carboxyl group in 11-MUA was activated by incubation in a 1:1 (v/v) mixture of EDC (0.2 M) and NHS (0.05 M) for 10 min, followed by washing with an immobilization buffer. For absorption of SA in 11-MUA, chips with the SAM surface were immersed in sodium acetate buffer (10 mM, pH 5.0) containing streptavidin at 40 μg/ml for 24 h. Residual NHS ester groups were blocked by incubating the chips in ethanolamine-HCl (pH 8.5) solution for 10 min. The chip was then incubated in PBS containing 40 μg/ml biotinylated probe for 30 min at room temperature, followed by a rinse with PBS (Fig. 1(a)) (Su et al., 2005).

The second approach is to immobilize the oligonucleotide probes directly on the gold surface with thiolated oligonucleotide, abbreviated HS-oligonucleotide, with has a HS-$(CH_2)_6$-attachment at the 5′ end. This approach has the benefits of a shorter processing time and has minimal effect on the surface density of the thiolated ssDNA monolayer (Pris et al., 2010). The SAM layer was patterned by immersing a cleaned SPR chip in a dilute solution of HS-oligonucleotide probe (40 μg/ml in PBS) for 30 min. Then the sensor chip was blocked by soaking it in MCH (5 mM in PBS) for 1 h at room temperature, followed by a rinse with PBS (Fig. 1(b)) (Milkani et al., 2010).

2.4. The preparation of target oligonucleotide

The target oligonucleotide was diluted in 400 μl PBS with 10-fold serial dilution from 0.5 nM to 0.5 pM. For construction of the basal level, PBS was added to the reaction chamber and retained for 3 min. The amplitude signal measured from 81 to

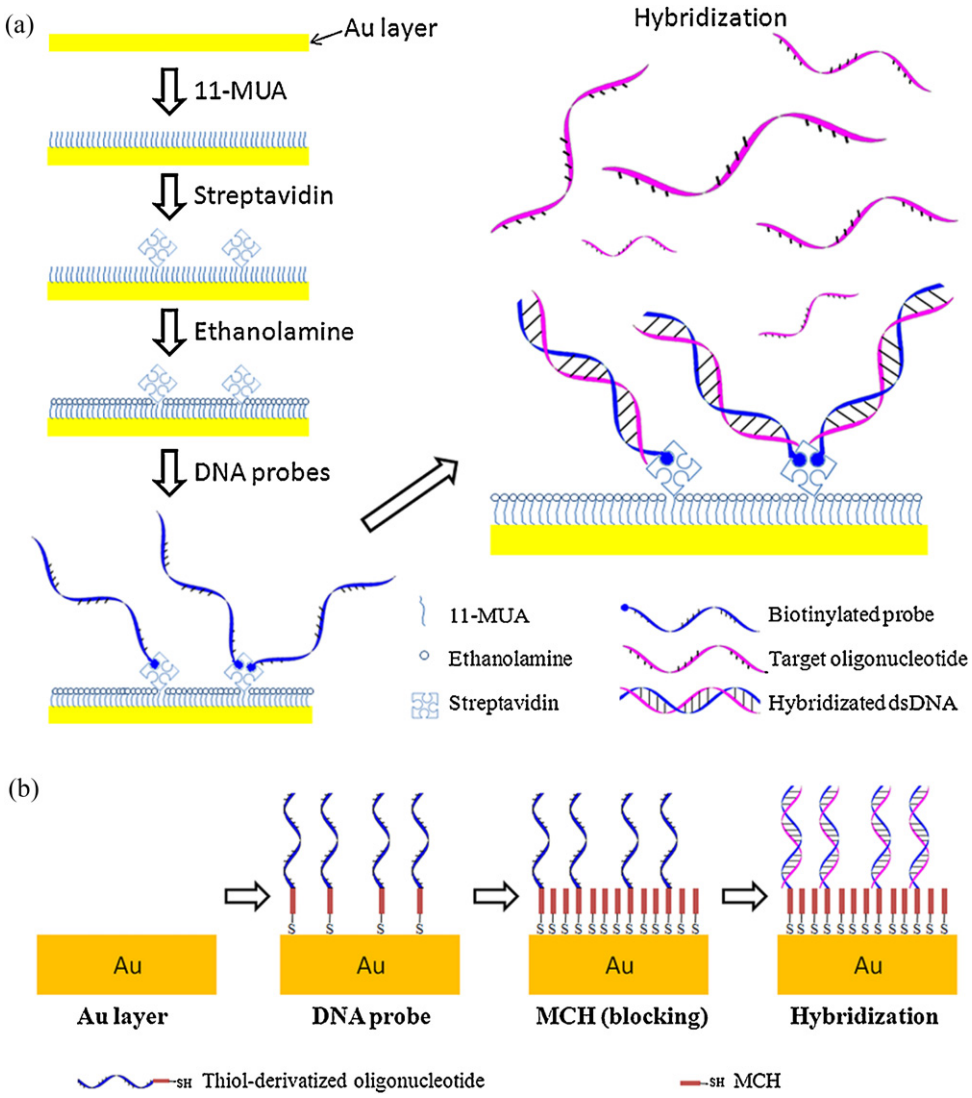

Fig. 1. Schema of immobilization of probe and hybridization of target oligonucleotides by using (a) the biotinylated oligonucleotide probe or (b) the thiolated oligonucleotide probe.

180 s was extracted to represent the basal level ($mean_I \pm S.D._I$). The analytes (diluted solutions of target oligonucleotides) were then applied to the reaction chamber and incubated for 30 min at room temperature. The sensor chip was washed with PBS to remove unbound target oligonucleotides. The amplitude during the period 2601–2700 s was extracted to represent the signal responding to hybridization of the target oligonucleotide ($mean_F \pm S.D._F$). The response was calculated according to the following formula:

$$\text{Response} = (\text{Mean}_F - \text{Mean}_I) \pm 3\sqrt{(\text{S.D.}_I)^2 + (\text{S.D.}_F)^2}$$

2.5. Measurement of affinity between oligonucleotides

The affinity between the probe and the target or the non-target oligonucleotide was measured by computer simulation and melting analysis. Computer simulation was performed using the software PerlPrimer (http://perlprimer.sourceforge.net/), which calculates the free energy between each pair of oligonucleotides.

A melting curve analysis was performed using a LightCycler 480 instrument (Roche). A double-stranded intercalating dye, SYBR Green I (Invitrogen), was used for monitoring oligonucleotide denaturation. SYBR Green I binds to the minor groove of a double-stranded oligonucleotide and generates intensive fluorescence with maximal signal at 533 nm. When the double-stranded DNA was denatured due to rising temperature, the fluorescence signal decreased along with the temperature change. The melting temperature (T_m) is defined as the temperature at which half of the double-stranded DNA denatures in solution. The T_m of each pair of oligonucleotides was measured by melting analysis on the LightCycler 480 instrument (Roche). The paired oligonucleotides at concentrations of 0.5 μM were hybridized in PBS containing 0.5X SYBR Green I for 5 min. Temperature of the reaction mixture was slowly increased to 95 °C. The intensity of SYBR green I signal was measured along with the temperature change. The fluorescence signal was measured along with the temperature change by the instrument.

3. Results and discussion

3.1. Construction of sensor chip

The surface of the chip after oligonucleotide immobilization is illustrated in Fig. 1(a). 11-MUA was assembled on the gold surface and conjugated with SA by NHS/EDC treatment. In order to achieve a better probe density in the sensing area, SA was immobilized

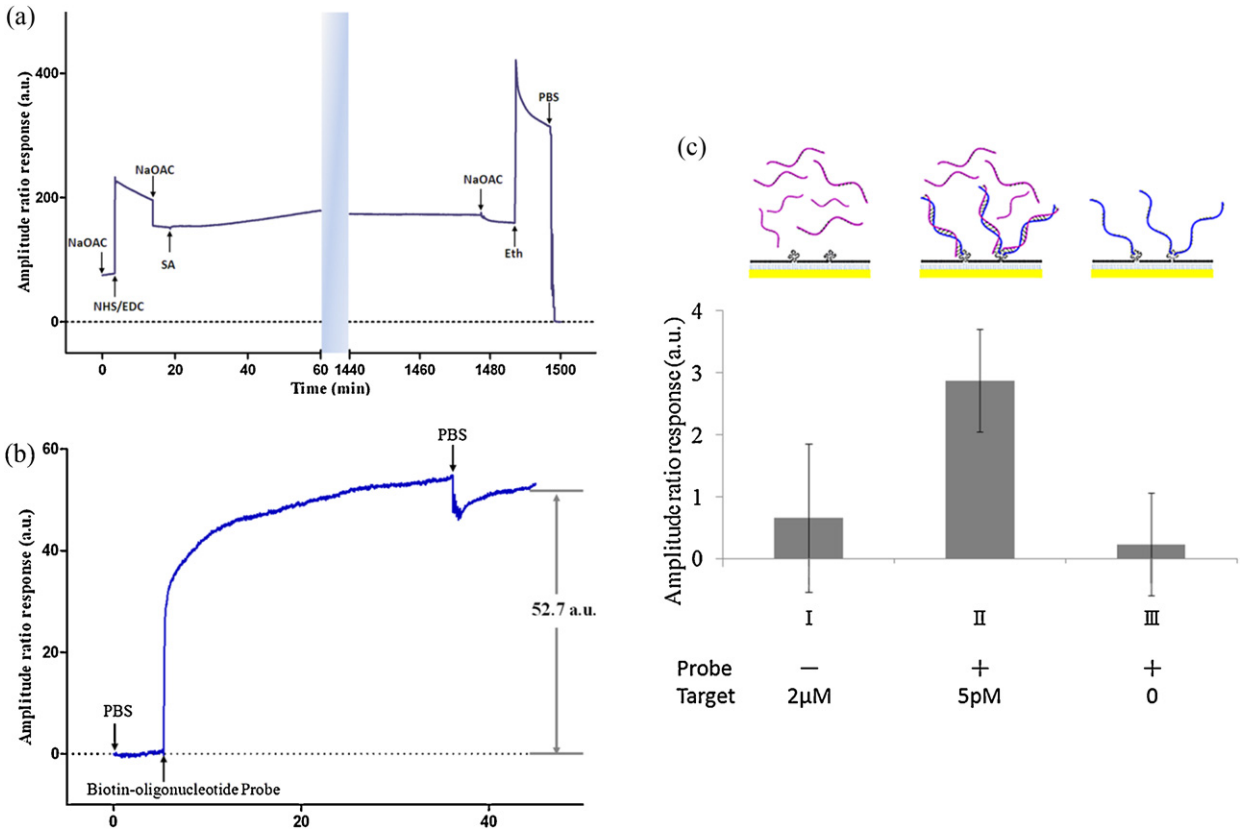

Fig. 2. (a) The amplitude ratio responses during surface modification. NaOAC represents sodium acetate buffer (pH 5.0); NHS, N-hydroxysuccinimide; EDC, 1-ethyl-3-(3-dimethylaminopropyl)-carbodiimide hydrochloride; SA, streptavidin; Eth, ethanolamine-HCl (pH 8.5); PBS, phosphate buffered saline (pH7.4). (b) The amplitude ratio responses of probe immobilization. (c) Comparison of PSPWB measurements for three situations of oligonucleotide hybridizatioin. I: oligonucleotide target without probe immobilization; II: oligonucleotide target and complementary probe hybridization; III: no oligonucleotide target with probe immobilization (PBS buffer only).

on the 11-MUA-modified surface via amide bonding followed by the specific attachment of biotin-labeled probes. Because SA has a high affinity for biotin ($K_d \sim 10^{-14}$ M) and one SA binds four biotin molecules, the biotinylated probe could bind efficiently to the streptavidin-coated surface.

The immobilization responses of SA and the probe oligonucleotide are illustrated in Fig. 2. Fig. 2(a) indicates the conjugation of SA with 11-MUA after NHS/EDC treatment. Acetate buffer (pH 5.0) was used as the immobilization buffer because, at low pH, the carboxyl group of 11-MUA and the amino group of SA retain higher activity, which enhanced the efficiency of the SA immobilization. Fig. 2(b) represents the binding curve of the oligonucleotide probe. In this measurement, when the biotinylated probe was injected into the chamber, it associated with the SA immediately and caused a rapid rise of the amplitude ratio response. PBS was then injected to wash away the unbound probe, resulting in a slight drop of the signal. The immobilization of the oligonucleotide probe therefore increased the amplitude ratio response by 52.7 a.u. (arbitrary unit) in this figure.

To demonstrate that the signals were generated from the hybridization between the probe and the target oligonucleotide, a sensor surface without probe (only SA layer attached on gold surface) was used as a control chip. When the target oligonucleotide (2 μM) was injected into the sensing chamber with the control chip, only a weak response (0.66 a.u.) was generated, as shown in Fig. 2(c)-I. After the measurement, the probe was added to the chip. The biotinylated probe was immobilized on the gold surface through association with SA. When the target was injected again, it generated an intense response (2.88 a.u.), whereas the concentration of the target was 5 pM in Fig. 2(c)-II. In Fig. 2(c)-III, no oligonucleotide binding was involved, and PBS was chosen as the control group with a background response at 0.23 a.u. From these results, it is obvious that PSPWB enables the detection of 15-mer oligonucleotide target hybridization with complementary probe at 5 pM in PBS. The signal level was increased 10 times in relation to the background response. As a result, a lower concentration of oligonucleotide target hybridized with probe can be anticipated.

3.2. Determination of detection limit

To determine the detection limit of a PSPWB, the amplitude ratio responses of a serially diluted targeted oligonucleotide were analyzed and fitted to a standard curve using a linear regression model. During detection, the paired *s* wave was monitored and used as a reference beam to correct the intensity fluctuation noise caused by instability of the laser beam. In these measurements, all the signals were stable over each processing time (45 min) with the coefficient of variation lower than 0.06%. Fig. 3 demonstrates that a linear relationship exists between the detected SPR signals and the concentrations of the target oligonucleotide. In order to assess the detection limit of the hybridization processes, the 15-mer target oligonucleotides at concentrations from 0.5 pM to 500 pM were measured for their amplitude ratio responses. The results were then fitted to a linear model with the following formula:

$$\mathrm{LOD} = \frac{\bar{x} + 3 \cdot \sigma}{m},$$

where $\bar{x}$ and σ are the mean and standard variation of the blank sample and m is the slope of the experimental calibration curve. The error bar of each point was defined as 3 times the standard deviation

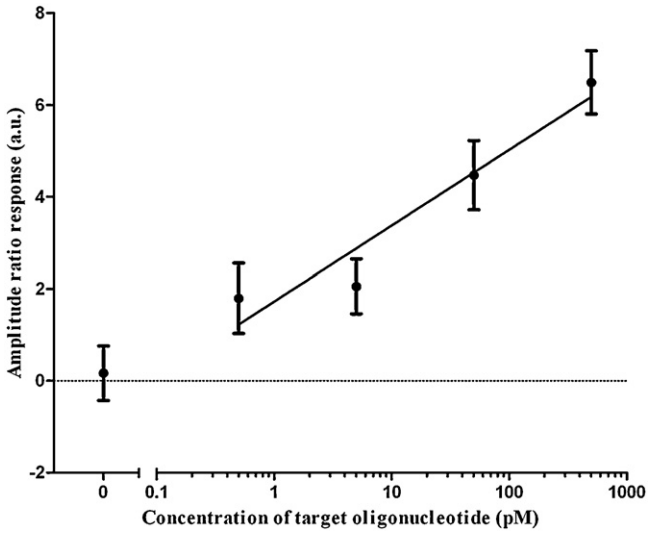

Fig. 3. Linearity of responses for different concentrations of analytes. The response for each concentration of oligonucleotide target is illustrated in this figure. The correlation coefficient (R^2) is 0.92950 and the error bar represents 3 standard deviations.

(SD). In this experiment, the response of the 0.5 pM target oligonucleotide (1.80 ± 0.76 a.u.) was significantly higher than the blank (0.17 ± 0.59 a.u.), suggesting that analytes at concentrations as low as 0.5 pM were detectable using this platform. According to the guidelines from IUPAC for calculating the limit of detection (LOD) (Jiang et al., 2005; Whelan et al., 2002), the LOD of our measurement was 0.5 pM.

It is apparent that this proposed method is more sensitive than the conventional SPR platforms for detecting un-labeled oligonucleotides: without modification, the traditional SPR has a detection limit for oligonucleotides at around 10 nM (Carrascosa et al., 2009). A few strategies have added some physical or optical modifications to increase the sensitivity, such as diffraction grating on the gold surface (Šípová et al., 2010) and the measurement of phase shift of *p*-polarized light (Halpern et al., 2011), with detection limits at 2 pM and 50 pM, respectively. Particle-labeling technologies may further increase the sensitivity for nucleic acid detection: for example, labeling with fluorescent dyes (Feng et al., 2011; Yu et al., 2009), gold nanoparticles (Storhoff et al., 2004; Bao et al., 2005) and quantum dots (Long et al., 2011; Han et al., 2011) can lower the detection limits to between 10 fM and 1 pM. However, the labeling technologies are not applicable in many situations, especially for detecting the oligonucleotide shorter than 25 nucleotides, as the oligonucleotide targets in biological samples are difficult to label and they are too short to be detected with a sandwich format (Bao et al., 2005).

Our PSPWB platform thus demonstrates superior features, consisting of high detection sensitivity and operational simplicity, due to the following characteristics: (1) PSPWB enables the reduction of noise spectrum via heterodyne interference and synchronized detection, (2) there is less fluctuation because the detected signals can be normalized via the algorithm of demodulated amplitude ratio of the signal and reference beams and (3) amplitude-sensitive detection by PSPWB has a wider dynamic range than the intensity detection used by conventional SPR biosensors.

Although PCR is still more sensitive than PSPWB for oligonucleotide detection, PSPWB provides an effective method for the detection of oligonucleotides without the requirement of enzymatic reactions, primer designation, and fluorescent labeling. For detecting highly abundant nucleic acid analytes, such as microRNAs, PSPWB can be a useful optical platform.

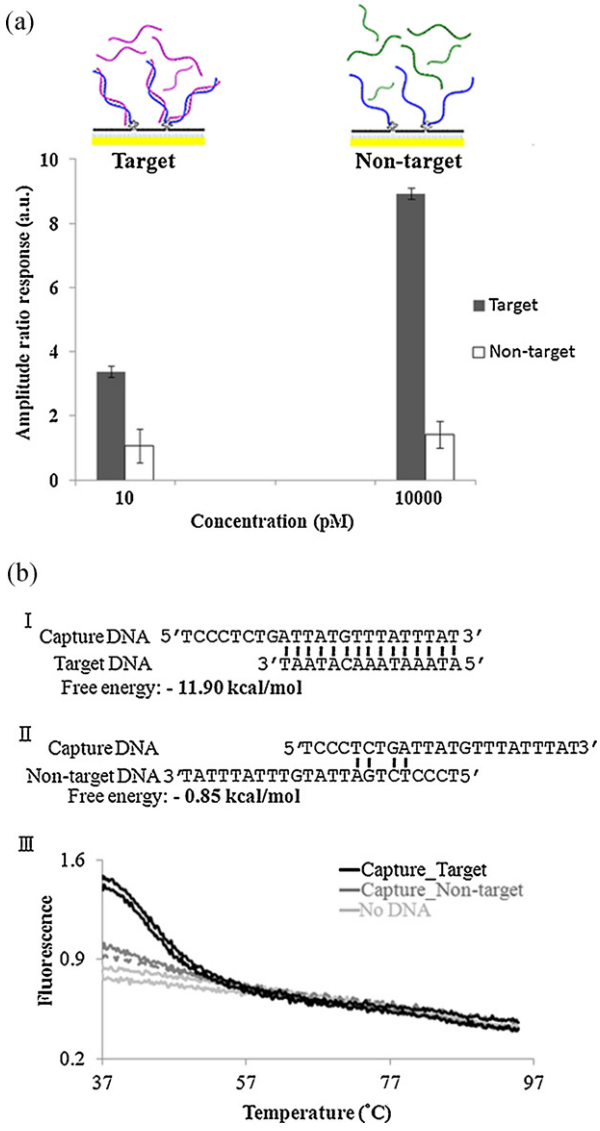

Fig. 4. (a) Responses showing complementary hybridization. Responses of oligonucleotide target (filled bar) are compared with non-targeted oligonucleotide (open bar). (b) Tests of affinity of target/non-target DNA towards capture DNA. Pairing model of target-capture DNA duplex (I) and non-target-capture DNA duplex (II) simulated by PerlPrimer are illustrated. The melting curve analysis (III) of the two duplexes is also demonstrated.

3.3. Validation of the oligonucleotide binding specificity

In order to demonstrate the selectivity for detecting an oligonucleotide with a specific sequence, a comparison between a 15-mer complementary target oligonucleotide and non-target oligonucleotide was made. Both oligonucleotides, at concentrations of 10 pM and 10 nM concentrations were tested for their responses after reaction with the immobilized probe (see Fig. 4(a)). The results revealed that the reactions of the complementary target and non-target can be clearly differentiated at 10 pM (3.37 a.u. versus 1.07 a.u.) or at 10 nM (8.93 a.u. versus 1.41 a.u.). In both concentrations, the non-target oligonucleotide which is not complementary to the immobilized probe only generated background signals apparently.

We also used two methods to estimate the affinity between the probe and the target or non-target oligonucleotides. The free energies between the captured probe and different target oligonucleotides were estimated by the software PerlPrimer (Fig. 4(b)-I

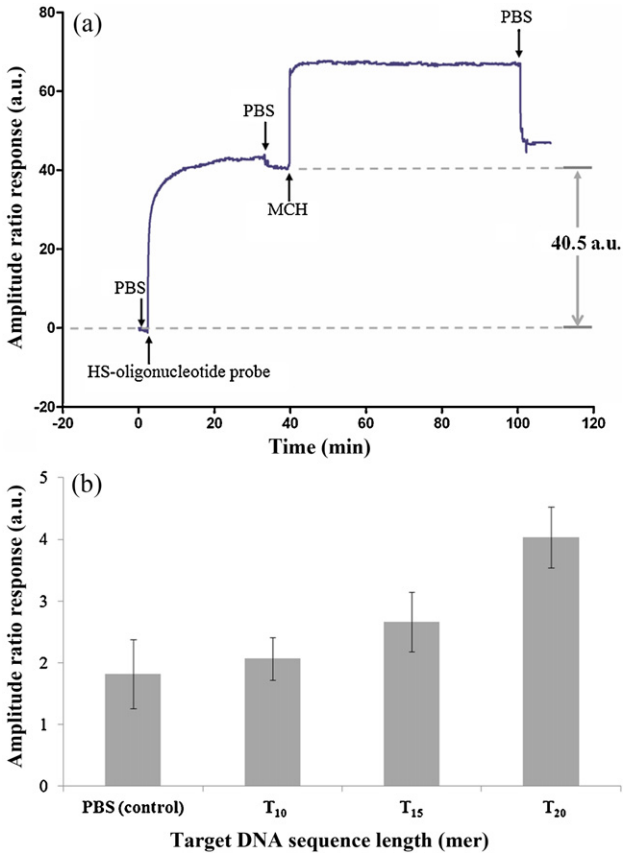

Fig. 5. (a) Amplitude response of probe immobilization by using thiolated oligonucleotide probe. (b) The amplitude ratio response of the binding of target oligonucleotides with different lengths (10-, 15-, and 20-mer, represented as T_{10}, T_{15}, and T_{20}, respectively). All target oligonucleotides were added at a concentration of 150 pM in PBS. Detection was performed at 25 °C.

and II).The free energies in the probe/target-oligonucleotide duplex and the probe/non-target-oligonucleotide duplex were −11.90 kcal/mol and −0.85 kcal/mol, respectively, indicating that the probe forms a strong association with the target oligonucleotide but not with the non-target oligonucleotide. Second, this speculation was proved by a melting curve analysis. Only the probe/target duplex generated a melting peak with a T_m value of 40 °C (Fig. 4(b)-III).

3.4. Length dependence of oligonucleotide target sequences

The sensitivity of PSPWB can also be demonstrated through perfectly matched hybridization of oligonucleotides with different length. The shorter oligonucleotide has lower molecular mass and lower affinity to the probe, making it more difficult to be detected. In this experiment, we used the thiolated probe to immobilize onto the sensor chip (see Fig. 2(b)). The binding response of oligonucleotide probe was depicted in Fig. 5(a). An apparently increase on amplitude ratio response assures the efficient immobilization of the probe. Then we proceeded the experiments by using target oligonucleotides, 10-mer (T_{10}), 15-mer (T_{15}), and 20-mer (T_{20}), binding with oligonucleotide probe sequentially. Fig. 5(b) shows the responses of perfect-match oligonucleotide targets of 10-, 15-, and 20-mer in length. All the targets were diluted at the same concentration of 150 pM concentration. From these results, we can see a clear difference of the detected demodulated amplitude ratio of SPR response. They are 2.07 a.u. (arbitrary unit), 2.66 a.u. and 4.03 a.u. with respect to 10-mer, 15-mer and 20-mer of target oligonucleotides. The magnitude of the amplitude ratio response of 10-mer is close to the level of the control (PBS buffer only), suggesting that the 10-mer oligonucleotide might not bind to the immobilized probe at room temperature (around 25 °C).

4. Conclusions

In this study, we have established a PSPWB-based optical platform for the detection of unlabeled oligonucleotides without any post-hybridization manipulation. The detection limit at 0.5 pM for the 15-mer oligonucleotide target indicates that PSPWB is more sensitive than conventional SPR systems. Further validation in our experiments demonstrates the credibility of the PSPWB responses on immobilization and hybridization, and the detection selectivity for discriminating complementary target and non-target oligonucleotides. We expect that PSPWB can be extended into the detection of oligonucleotide biomarkers, such as microRNAs in the biomedical samples.

Acknowledgments

This research was partially supported by the National Science Council of Taiwan (NSC98-2221-E-182-063-MY3, NSC98-2221-E-182-064-MY3), and the Ministry of Education, aiming from the Top University Plan (EMRPD 1A0751). The support from Healthy Aging Research Center (HARC) in Chang Gung University is also appreciated.

Appendix A. Supplementary data

Supplementary data associated with this article can be found, in the online version, at doi:10.1016/j.bios.2012.03.014.

References

Ananthanawat, C., Vilaivan, T., Mekboonsonglarp, W., Hoven, V.P., 2009. Biosens. Bioelectron. 24, 3544–3549.
Bao, Y.P., Huber, M., Wei, T.F., Marla, S.S., Storhoff, J.J., Müller, U.R., 2005. Nucleic Acids Res. 33, e15.
Carrascosa, L.G., Calle, A., Lechuga, L.M., 2009. Anal. Bioanal. Chem. 393, 1173–1182.
Chiang, Y.L., Lin, C.H., Yen, M.Y., Su, Y.D., Chen, S.J., Chen, H.F., 2009. Biosens. Bioelectron. 24, 1905–1910.
Chou, C., Wu, H.T., Huang, Y.C., Kuo, W.C., Chen, Y.L., Kuo, W.C., 2006. Opt. Express 14, 4307–4315.
D'Agata, R., Corradini, R., Ferretti, C., Zanoli, L., Gatti, M., Marchelli, R., Spoto, G., 2010. Biosens. Bioelectron. 25, 2095–2100.
D'Agata, R., Corradini, R., Grasso, G., Marchelli, R., Spoto, G., 2008. ChemBioChem 9, 2067–2070.
Endo, T., Ikeda, D., Kawakami, Y., Yanagida, Y., Hatsuzawa, T., 2010. Anal. Chim. Acta 661, 200–205.
Feng, C.L., Yin, M., Zhang, D., Zhu, S., Caminade, A.M., Majoral, J.P., Müllen, K., 2011. Macromol. Rapid Commun. 32, 679–683.
Gifford, L.K., Sendroiu, I.E., Corn, R.M., Lupták, A., 2010. J. Am. Chem. Soc. 132, 9265–9267.
Gorshkova, I.I., Rausch, J.W., Le Grice, S.F.J., Crouch, R.J., 2001. Anal. Biochem. 291, 198–206.
Halpern, A.R., Chen, Y., Corn, R.M., Kim, D., 2011. Anal. Chem. 83, 2801–2806.
Han, H., Zylstra, J., Maye, M.M., 2011. Chem. Mater. 23, 4975–4981.
Hiep, H.M., Saito, M., Nakamura, Y., Tamiya, E., 2010. Anal. Bioanal. Chem. 396, 2575–2581.
Jiang, T., Minunni, M., Wilson, P., Zhang, J., Turner, A.P.F., Mascini, M., 2005. Biosens. Bioelectron. 20, 1939–1945.
Kick, A., Bönsch, M., Katzschner, B., Voigt, J., Herr, A., Brabetz, W., Jung, M., Sonntag, F., Klotzbach, U., Danz, N., Howitz, S., Mertig, M., 2010. Biosens. Bioelectron. 26, 1543–1547.
Kuo, W.C., Chou, C., Wu, H.T., 2003. Opt. Lett. 28, 1329–1331.
Kuo, Y.C., Ho, J.H., Yen, T.J., Chen, H.F., Lee, O.K.S., 2011. PLoS ONE 6, e22382.
Lin, M.T., Tseng, L.H., Kamiyama, H., Kamiyama, M., Lim, P., Hidalgo, M., Wheelan, S., Eshleman, J.R., 2010. Biotechniques 48, 351–355.
Liu, G., Wan, Y., Gau, V., Zhang, J., Wang, L., Song, S., Fan, C., 2008. J. Am. Chem. Soc. 130, 6820–6825.
Long, F., Wu, S., He, M., Tong, T., Shi, H., 2011. Biosens. Bioelectron. 26, 2390–2395.
Luan, Q., Xue, Y., Yao, X., Lu, W., 2010. Analyst 135, 414–418.
Majka, J., Speck, C., 2007. Adv. Biochem. Eng. Biotechnol. 104, 13–36.
Milkani, E., Morais, S., Lambert, C.R., McGimpsey, W.G., 2010. Biosens. Bioelectron. 25, 1217–1220.

Nelson, B.P., Grimsrud, T.E., Liles, M.R., Goodman, R.M., Corn, R.M., 2001. Anal. Chem. 73, 1–7.
Okumura, A., Sato, Y., Kyo, M., Kawaguchi, H., 2005. Anal. Biochem. 339, 328–337.
Pollet, J., Delport, F., Janssen, K.P.F., Jans, K., Maes, G., Pfeiffer, H., Wevers, M., Lammertyn, J., 2009. Biosens. Bioelectron. 25, 864–869.
Pris, A.D., Ostrowski, S.G., Garaas, S.D., 2010. Langmuir 26, 5655–5660.
Raz, S.R., Bremer, M.G.E.G., Haasnoot, W., Norde, W., 2009. Anal. Chem. 81, 7743–7749.
Shumaker-Parry, J.S., Zareie, M.H., Aebersold, R., Campbell, C.T., 2004. Anal. Chem. 76, 918–929.
Šípová, H., Zhang, S., Dudley, A.M., Galas, D., Wang, K., Homola, J., 2010. Anal. Chem. 82, 10110–10115.
Storhoff, J.J., Marla, S.S., Bao, P., Hagenow, S., Mehta, H., Lucas, A., Garimella, V., Patno, T., Buckingham, W., Cork, W., Müller, U.R., 2004. Biosens. Bioelectron. 19, 875–883.
Su, L.C., Chen, R.C., Li, Y.C., Chang, Y.F., Lee, Y.J., Lee, C.C., Chou, C., 2010. Anal. Chem. 82, 3714–3718.
Su, X., Neo, S.J., Peh, W.Y.X., Thomsen, J.S., 2008. Anal. Biochem. 376, 137–143.
Su, X., Ying, Wu, Y.J., Robelek, R., Knoll, W., 2005. Langmuir 21, 348–353.
Tsoi, P.Y., Yang, M., 2004. Biosens. Bioelectron. 19, 1209–1218.
Wang, Y., Zhu, X., Wu, M., Xia, N., Wang, J., Zhou, F., 2009. Anal. Chem. 81, 8441–8446.
Wark, A.W., Lee, H.J., Qavi, A.J., Corn, R.M., 2007. Anal. Chem. 79, 6697–6701.
Wegner, G.J., Lee, H.J., Marriott, G., Corn, R.M., 2003. Anal. Chem. 75, 4740–4746.
Whelan, R.J., Wohland, T., Neumann, L., Huang, B., Kobilka, B.K., Zare, R.N., 2002. Anal. Chem. 74, 4570–4576.
Wong, C.L., Ho, H.P., Suen, Y.K., Kong, S.K., Chen, Q.L., Yuan, W., Wu, S.Y., 2008. Biosens. Bioelectron. 24, 606–612.
Wu, L., Zhang, Q., Su, L., Huang, M., Zhao, J., Yang, M., 2007. Sens. Actuator B: Chem. 122, 243–252.
Yu, Y., Feng, C., Caminade, A.M., Majoral, J.P., Knoll, W., 2009. Langmuir 25, 13680–13684.